RESEARCH ARTICLE

Comparative Analysis of Smart Meter Testing According to International Standards with AI-Based Methods for Anomaly Detection

Saša Aleksandrov[1,*]

[1] R&D Department, EWG DOO Beograd, Niš 18106, Serbia

Abstract

Standard type verification of three-phase smart meters is performed under idealized balanced test conditions that do not fully reproduce the current unbalance, single-phase loading and voltage deviations found on real distribution networks, so that a channel-specific calibration fault can pass undetected. This paper presents a methodology combining standard IEC 62052-11 and EN 50470-3 verification with an extended set of near-real-network test conditions (unbalanced current distribution, single-phase loading, and voltage deviation from nominal), together with a statistical/machine-learning screening step applied to aggregated laboratory verification results and used to flag units for targeted extended validation. Three three-phase static meters were analyzed: two units flagged by the screening procedure and one reference unit. Under standard balanced testing all three units remained within their declared accuracy class, but under extended single-phase loading on one specific current channel the two flagged units exhibited systematic registration errors of up to approximately 4%, traced to an incorrectly recorded calibration coefficient on that channel; the reference unit remained within tolerance throughout. The results show that screening of aggregated verification data can identify meters with hidden channel-specific faults that standard balanced verification alone does not reveal, and support extending routine Type C verification with a small set of unbalanced/single-phase test points. The primary contribution of this work is the extended verification methodology and its validation on a real production case; the AI-assisted screening is employed as a triggering mechanism.

Keywords: anomaly detection, machine learning, metrological validation, smart meter.

1 Introduction

The evolution of electricity distribution systems, from Edison's early direct-current networks to today's smart grids, has been marked by continuous advances in metering technology. As a core component of the modern grid, smart meters provide real-time data on energy consumption and demand, which distribution system operators (DSOs) rely on to optimize network operation, manage demand and improve reliability. They enable dynamic pricing, remote monitoring and

Submitted: 19 July 2026
Revised: 02 September 2026
Accepted: 08 September 2026
Published: 12 September 2026

Vol. 2, **No.** 3, 2026.
10.62762/TEPNS.2026.407661

***Corresponding author:**
Saša Aleksandrov
alsasa@ewg.rs

Citation
Aleksandrov, S. (2026). Comparative Analysis of Smart Meter Testing According to International Standards with AI-Based Methods for Anomaly Detection. *ICCK Transactions on Electric Power Networks and Systems*, 2(3), 149–160.

control, and support the integration of renewable generation, in line with EU policy objectives such as the "Fit for 55" package [1] and the REPowerEU plan [2], both of which depend on accurate metering data for the monitoring and verification of energy savings and demand-side flexibility at the consumer level.

Reliable measurement, security and interoperability are prerequisites for these functions, since smart meters must communicate seamlessly across heterogeneous devices and networks while their accuracy is trusted for billing purposes. Testing of active and reactive energy, power, voltage, current and frequency at various loads and power factors is carried out under both steady-state and dynamic conditions and evaluated against international standards [3–5], covering systematic and random error components, calibration drift, electromagnetic susceptibility and firmware-related faults. This raises the question of whether standard verification procedures adequately exercise a meter's measurement system under conditions representative of real network operation.

A recurring limitation of standard verification procedures is that they are performed under idealized signal conditions that do not fully reproduce the imbalance, distorted power factor and voltage spread observed at real metering points, and consequently do not fully exercise every state of a meter's signal-processing chain [6]. Complementary experimental work has developed open-source research platforms for smart-grid metering and carried out systematic intercomparison of commercially available smart-meter technologies under controlled laboratory conditions, illustrating the diversity of measurement performance that routine verification procedures must be capable of resolving [7]. A substantial body of machine-learning literature separately addresses anomaly and fault detection from smart-meter data, ranging from isolation-forest and autoencoder-based screening and benchmarking of statistical, unsupervised and deep-learning models [8] to broader surveys of artificial-intelligence techniques for smart-grid anomaly detection [9, 10]. Power-quality-oriented anomaly screening of smart-meter data has likewise been proposed as a complement to periodic verification [11], and studies of static energy meters under non-standard electrical conditions confirm that steady-state accuracy under standard test points does not necessarily generalize to all real operating conditions [12]. Taken together, this literature indicates that (a) standard verification test points may not exercise every relevant operating state of a meter's measurement systems, and (b) statistical/machine-learning screening of accuracy data is an active but still-maturing field, generally applied to consumption time series rather than to the structured, standards-based verification datasets produced by accredited testing laboratories. This gap—the lack of a demonstrated route from routine laboratory verification data, via statistical/machine-learning screening, to targeted extended testing capable of confirming a hidden channel-specific fault—is addressed by the present paper.

This paper presents the testing methodology applied by EWG (a Serbian smart-meter manufacturer, whose accredited inspection body is EWG Control – Bor), compares it against the requirements of IEC 62052-11 and EN 50470-3, and reports validation results obtained on three three-phase static meters under both standard and extended test conditions designed to approximate real network operating states. It further describes how statistical/AI-assisted screening of the laboratory's aggregated verification results was used to identify two units with a systematic calibration fault that standard testing alone did not flag, and presents and discusses the resulting measurements. The main contribution is an experimentally validated demonstration that a channel-specific calibration fault, invisible under standard balanced verification, can be reliably exposed by a small set of unbalanced/single-phase extended test points and independently flagged by screening of routine verification data; a detailed description of the screening algorithm itself—including its detection sensitivity and false-positive rate—is left to a dedicated follow-up paper. The AI-assisted screening serves as the triggering mechanism that directed attention to the affected units, with the algorithm's internal details deferred to that follow-up work.

The remainder of the paper is organized as follows: Section 2 reviews the relevant international and national regulatory framework, together with the role of the EWG accredited inspection body; Section 3 describes the extended test methodology; Section 4 presents the AI-assisted anomaly-screening approach; Section 5 reports and discusses the measurement results; and Section 6 concludes the paper.

2 Standards and Regulatory Framework

2.1 International Framework

Internationally, type approval and periodic verification of static electricity meters are harmonized primarily under the IEC 62052/62053 series. Technical requirements are specified in IEC 62052-11:2022, *General requirements, tests and test conditions — Part 11: Metering equipment* [3], complemented by the IEC 62053 series for the accuracy-class requirements of active- and reactive-energy static meters [4]. In the European Union, these requirements are further specified in EN 50470-3:2022 for active-energy static meters [5], harmonized with the EU Measuring Instruments Directive 2014/32/EU (MID) [13].

2.2 National (Serbian) Framework

Type verification and periodic/first verification of electricity meters in Serbia are carried out under the national Regulation on the Verification of Active Electrical Energy Meters of Accuracy Classes A, B and C [14] ("Sl. glasnik RS", No. 14/2024), harmonized with the MID [13].

2.3 EWG Accredited Inspection Body

EWG Control – Bor is an organizational unit of EWG doo Belgrade, accredited by the Accreditation Body of Serbia (ATS) as a type C inspection body under ISO/IEC 17020:2012 [15] (Accreditation Certificate No. 159/2024, 28 February 2024). It is authorized by the Directorate for Measures and Precious Metals (Ministry of Economy, Decision No. 393-4/1-02-1068/1, 20 May 2024) to perform first, periodic and extraordinary verification of single- and three-phase active- and reactive-energy meters, for direct, semi-indirect and indirect connection, covering both EWG's own production and meters produced by other manufacturers.

Final-inspection testing of multifunction energy meters follows EWG's internal, non-published quality-system procedure UP.063 (issue 3, 8 April 2025), itself based on the national regulations and standards listed above.

3 Test Methodology

3.1 Objectives

The testing program aims to: (i) validate accuracy, reliability and repeatability under standard test conditions; (ii) assess performance under load, voltage and network conditions that more closely resemble those found on the distribution network; and (iii) evaluate whether statistical/AI-based screening of aggregated laboratory results can flag meters requiring closer inspection before they leave the production or verification process.

3.2 Standard (Factory) and Extended Test Points

General test conditions for accuracy testing of electricity meters are defined in IEC 62052-11:2022 (Clause 7.1) [3]. Under these conditions, EN 50470-3:2022, Clause 7.9 [5] specifies the permissible error limits for variation of current and power factor, referenced to the characteristic currents of EN 50470-1, Clause 3.5: starting current I_{st}, minimum current I_{min}, transitional current I_{tr}, reference current I_{ref} and maximum current I_{max} (all currents in A, voltages in V). The test points listed in Tables 1–5 were derived from these clauses and from EWG's internal instruction UP.063; for each test condition below, the factory (standard) point set required by the regulation is compared with the extended point set applied by EWG for this work.

For the regular balanced three-phase procedure, at rated voltage $3 \times 230/400$ V with equal current on all three phases, factory verification checks the current/power-factor combinations listed in Table 1. The extended procedure adds further combinations at the same and additional current levels—including inductive and capacitive power factor at every point—also listed in Table 1.

Table 1. Standard (factory) vs. extended test points — balanced three-phase load.

Factory current	Factory $\cos\varphi$	Extended current	Extended $\cos\varphi$
I_{st}	1	—	—
I_{min}	1	I_{min}	1
I_{tr}	1, 0.5L	I_{tr}	1, 0.5L, 0.8C
50% I_{ref}	1, 0.5L	20% I_{ref}	1, 0.5L, 0.8C
I_{ref}	1, 0.5L, 0.8C	I_{ref}	1, 0.5L, 0.8C
I_{max}	1, 0.5L	$2 \times I_{ref}$	1, 0.5L, 0.8C

The regular single-phase load procedure, performed at the same rated three-phase voltage, checks only the reference current at unity power factor, applied in turn to each phase. The extended procedure instead exercises each phase individually across four current levels and three power factors, as summarized in Table 2. This extended single-phase point set is also the basis for the L2 test discussed in Section 5, where confining the current to a single phase revealed a systematic registration fault that was not clearly visible under balanced loading.

IEC 62052-11:2022, Clause 9.4.5 [3] (Interruption of the phase voltage) was implemented as an extended test in which voltage and current are present on only one phase at a time, the other two phases being de-energized as if interrupted. Table 3 lists the corresponding test points, applied in turn to phases

Table 2. Standard (factory) vs. extended test points — single-phase load.

Phase	Factory current / $\cos\varphi$	Extended currents	Extended $\cos\varphi$
L1	I_{ref}, 1	I_{tr}, 20% I_{ref}, I_{ref}, $2 \times I_{\text{ref}}$	1, 0.5L, 0.8C
L2	I_{ref}, 1	I_{tr}, 20% I_{ref}, I_{ref}, $2 \times I_{\text{ref}}$	1, 0.5L, 0.8C
L3	I_{ref}, 1	I_{tr}, 20% I_{ref}, I_{ref}, $2 \times I_{\text{ref}}$	1, 0.5L, 0.8C

L1, L2 and L3.

Table 3. Extended test points — interruption of phase voltage (single active phase).

Active phase	Voltage	Current	$\cos\varphi$
L1	230 V	0.5, 1, 5, 10 A	1, 0.5L, 0.8C
L2	230 V	0.5, 1, 5, 10 A	1, 0.5L, 0.8C
L3	230 V	0.5, 1, 5, 10 A	1, 0.5L, 0.8C

IEC 62052-11:2022, Clause 9.4.3 [3] (Voltage variations) specifies the test voltage range; this was implemented with the extended voltage set given in Table 4, applied at three current levels and three power factors on a balanced three-phase load.

Table 4. Extended test points — voltage variation.

Three-phase voltage	Current	$\cos\varphi$
3×184 V	$3 \times 0.5, 3 \times 5, 3 \times 10$ A	1, 0.5L, 0.8C
3×207 V	$3 \times 0.5, 3 \times 5, 3 \times 10$ A	1, 0.5L, 0.8C
3×253 V	$3 \times 0.5, 3 \times 5, 3 \times 10$ A	1, 0.5L, 0.8C
3×264.5 V	$3 \times 0.5, 3 \times 5, 3 \times 10$ A	1, 0.5L, 0.8C

Additional test points, shown in Table 5, are defined in order to bring the test conditions closer to those of the real distribution network. At a balanced voltage of $3 \times 230/400$ V, the currents per phase differ (three combinations); a variant was also tested in which the currents and voltages take different values on each phase.

Table 5. Extended test points — voltage and current variation.

Three-phase voltage	Current	$\cos\varphi$
3×230 V	$0.5-5-10$ A	1
3×230 V	$10-0.5-5$ A	1
3×230 V	$5-10-0.5$ A	1
$184-230-254$ V	$0.5-5-10$ A	1
$184-230-254$ V	$10-5-0.5$ A	1

Taken together, factory verification followed IEC 62052-11:2022 Clause 7.1 [3] and EN 50470-3:2022 Clause 7.9 [5], while the extended procedure broadened these same clauses, together with Clauses 9.4.3 and 9.4.5 [3], to the near-real-network conditions summarized in Tables 1–5.

3.3 Rationale for the Extended Test Points

Standard measuring points rarely reproduce actual conditions at the metering point: three-phase voltages are seldom identical, loading is rarely symmetrical across phases, and the power factor varies continuously. The extended point set summarized in Tables 1–5 was designed to approximate these real network states more closely than factory verification alone, and, as shown in Section 5, was able to expose a fault that the factory point set did not.

3.4 Measurement Equipment and Sample Selection

Reference measurements were performed with a GFUVE GF302D reference standard [16], a three-phase test bench with optical pulse pick-up on the meters under test, rated at 600 VA per phase, accuracy class 0.1, and a maximum test current of 12 A, connected to a PC for automated test-sequence execution and data logging.

Three production three-phase static meters were selected: two units flagged by the screening procedure described in Section 4 (identified here as #22 and #34), and one unit used as a reference, in the normal error range (#33).

4 AI-Assisted Anomaly Screening as a Triggering Mechanism

Beyond the individual extended tests described in Section 3, the error values recorded during routine verification of each meter—at the standard current and power-factor combinations of Table 1—were aggregated across the population of units processed in the EWG laboratory and treated as a multivariate feature vector per meter (registration error at each standard test point, at each power factor). A statistical baseline screening procedure was applied to this dataset: for each standard test point and power factor, deviation of a unit's error from the batch mean beyond a fixed number of standard deviations was used to flag meters whose overall error pattern across test points deviated significantly from the otherwise-passing population, without requiring any single test point to individually exceed the standard's tolerance limits. This threshold-based approach was sufficient to flag meters #22 and #34 in the present case, despite both

Table 6. Error (%), standard balanced 3-phase test, $\cos\varphi = 1$, 0.5 inductive, 0.8 capacitive.

Current	0.25 A	0.5 A			1 A			5 A			10 A		
Meter	1	1	0.5L	0.8C	1	0.5L	0.8C	1	0.5L	0.8C	1	0.5L	0.8C
First measurement													
#22	0.497	0.535	−0.074	0.774	0.563	−0.046	0.801	0.560	−0.090	0.833	0.546	−0.147	0.829
#34	0.424	0.470	−0.307	0.777	0.493	−0.268	0.797	0.492	−0.311	0.838	0.493	−0.364	0.849
#33 (ref.)	−0.138	−0.096	−0.046	−0.161	−0.092	−0.023	−0.136	−0.081	−0.043	−0.106	−0.098	−0.087	−0.102
Repeated measurement (repeatability check)													
#22	0.491	0.532	−0.087	0.763	0.556	−0.055	0.788	0.547	−0.097	0.822	0.543	−0.151	0.831
#34	0.432	0.474	−0.311	0.772	−0.265[†]	−0.265	0.800	0.498	−0.309	0.832	0.482	−0.364	0.850
#33 (ref.)	−0.132	−0.096	−0.063	−0.164	−0.029[†]	−0.029	−0.136	−0.081	−0.044	−0.112	−0.092	−0.097	−0.104

[†]Single value recorded for both $\cos\varphi = 1$ and 0.5 inductive at 1 A in the repeated run; instrument log confirmed a single-point capture for this combination.

units passing every individual standard test point (Table 6).

Figure 1 summarizes this workflow: (1) standard factory verification of each unit against IEC 62052-11 / EN 50470-3 [3, 5]; (2) aggregation of the resulting per-point error values into the laboratory database; (3) construction of a per-meter feature vector and statistical/machine-learning screening against the population of results; (4) flagging of units whose pattern deviates from the population; (5) targeted extended testing (Tables 1–5) on flagged units together with a reference unit; and (6) root-cause analysis and, where confirmed, correction of the calibration coefficient, with a feedback path back into production/calibration.

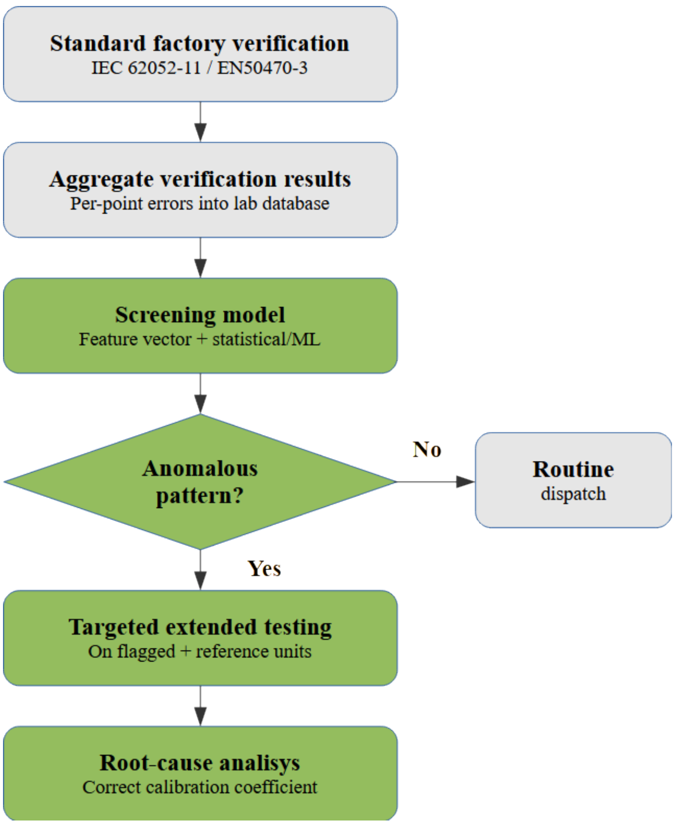

Figure 1. AI-assisted anomaly-screening workflow.

Meters #22 and #34 were flagged by this procedure despite passing every individual standard test point (Table 6), and were consequently directed toward the extended single-phase and voltage-variation test sequence reported in Section 5. A full description of the screening method—feature engineering, model selection, threshold calibration, and validation of its detection sensitivity and false-positive rate against a larger population of laboratory results—is left to a dedicated follow-up paper; here it is used only as the trigger that directed the two flagged meters (#22, #34) toward the extended testing reported in Section 5, which subsequently traced the deviation to an incorrectly recorded calibration coefficient on one current channel.

Beyond the statistical-baseline implementation used in the present study, EWG plans to extend the laboratory's screening pipeline with a layered architecture combining three complementary stages: (1) the statistical baseline described above, retained as a fast, transparent first pass; (2) an Isolation Forest stage [8] operating on the full multivariate feature vector to isolate units whose overall error pattern deviates from the bulk of the population without relying on any single fixed threshold; and (3) an autoencoder stage [8], trained to reconstruct the error patterns typical of verified, in-tolerance meters, to flag units with elevated reconstruction error, capturing subtler, non-linear deviations that the first two stages may not detect on their own. Each stage operates on the same per-meter feature vector already recorded in EWG's standard verification reports (error at each of I_{min}, I_{tr}, I_{ref} and I_{max}, at $\cos\varphi = 1$, 0.5 inductive and 0.8 capacitive), so that no additional data collection beyond routine laboratory record-keeping would be required for its deployment. This staged combination follows the general class of approaches surveyed in [8–10] and is intended for introduction into the EWG Control laboratory's routine data pipeline; its detailed design, feature engineering, hyperparameter

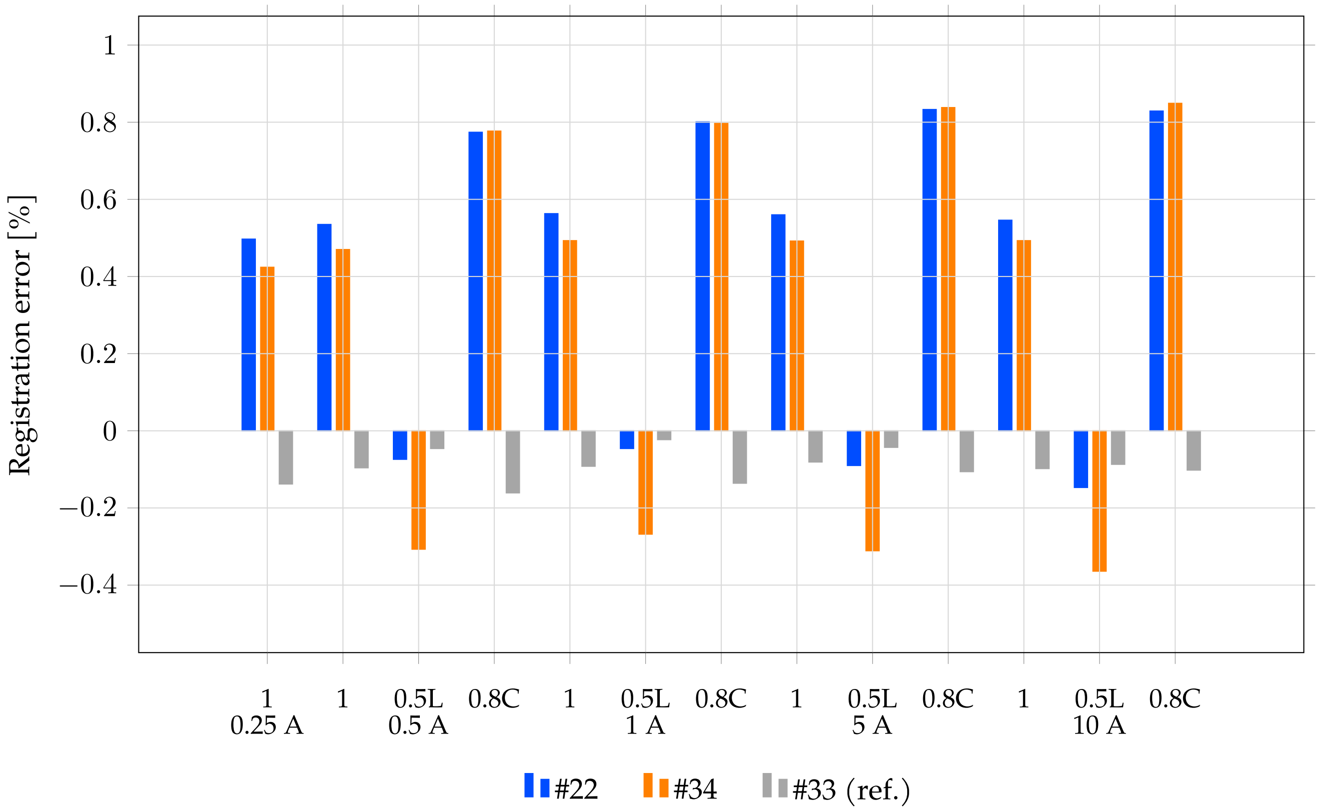

Figure 2. Registration error under the standard balanced three-phase test for each of the three meters (first measurement).

calibration, and a systematic evaluation of detection sensitivity and false-positive rate against a larger population of laboratory results are left to a dedicated follow-up paper.

5 Results and Discussion

Having identified meters #22 and #34 through the AI-assisted screening procedure described in Section 4, this section presents the extended experimental testing (Tables 1–5) used to confirm and characterize the underlying fault through direct measurement.

Table 6 summarizes the registration error (%) of the three meters under the standard balanced three-phase test ($\cos\varphi = 1$, 0.5 inductive and 0.8 capacitive) at representative currents. All three meters, including reference meter #33, remain within the declared accuracy class across the full standard point set; the deviation between #22/#34 and the reference is only a few tenths of a percent, consistent with normal unit-to-unit calibration spread rather than a metrological fault.

The same test was repeated under the same conditions in order to demonstrate repeatability—that is, to confirm that the variation (the deviation of errors between two consecutive measurements) is negligible.

Figure 2 shows the registration errors of the three meters at all standard balanced test points; the errors of meters #22 and #34 remain well below the allowed values under EN 50470-3 [5] and are difficult to distinguish in the official test-lab report. Notably, the errors at inductive load are smaller than at $\cos\varphi = 1$ and capacitive load, approaching the reference meter's values, while at capacitive load the spread across power factors reaches roughly one percentage point—still well inside the declared accuracy class under standard balanced loading.

Figure 3 shows the results of the first and repeated test of the three meters under the standard balanced load conditions at power factor $\cos\varphi = 1$. For meters #22 and #33 the error differences between the first and repeated measurements are negligibly small across all current levels. For meter #34 at 1 A, a single-point capture anomaly was recorded during the repeated run (see Table 6, note †); all remaining points confirm good repeatability. The situation is the same with inductive and capacitive loads.

This confirms objective (i) of Section 3.1—validating baseline accuracy and repeatability under standard test conditions before proceeding to extended, closer-to-real-network points.

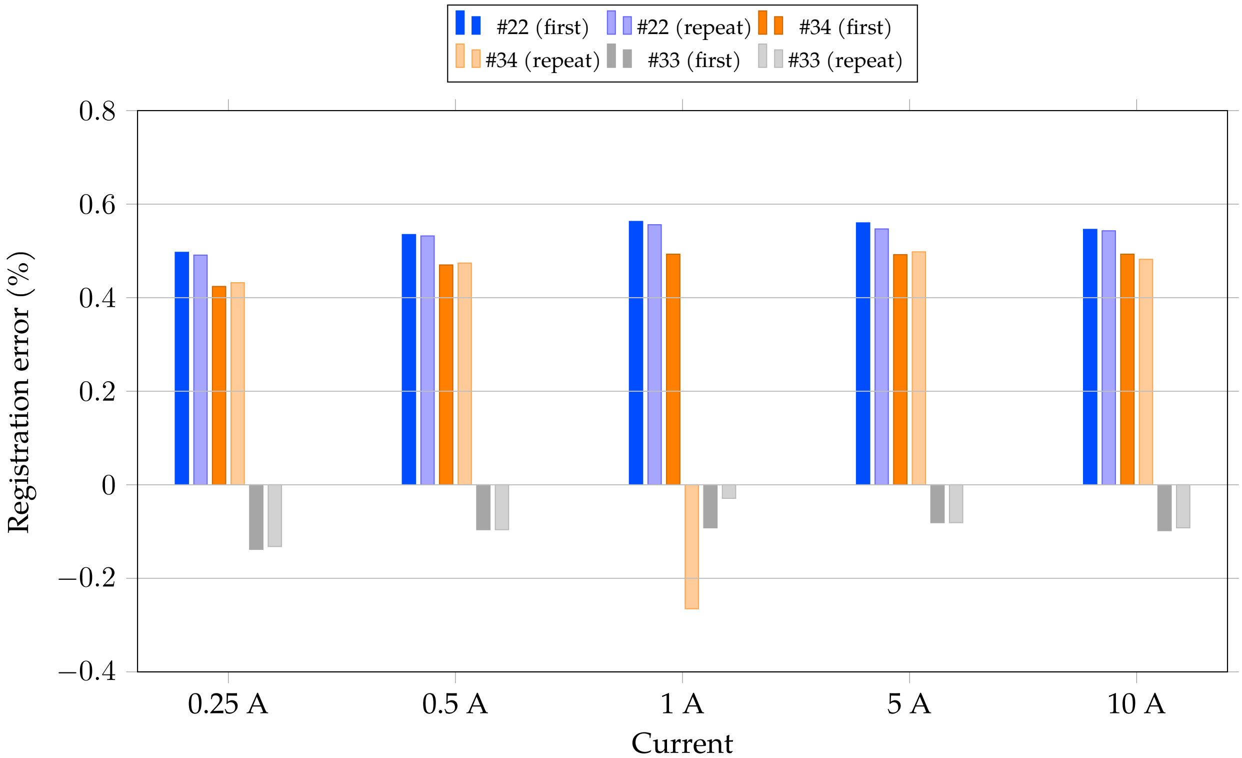

Figure 3. Registration error under the standard balanced three-phase test at $\cos\varphi = 1$: comparison of the first and repeated measurements. The anomalous value for #34 at 1 A in the repeated run is explained in Table 6 (note †).

A markedly different picture emerges under the extended single-phase load condition, where current flows through one specific phase (L2) only while the other two phases carry no current. Table 7 shows that, for this condition, meters #22 and #34 register errors between $+1.6\%$ and $+1.7\%$ for $\cos\varphi = 1$ and up to $+2.8\%$ for $\cos\varphi = 0.8$ capacitive load, while reference meter #33 remains within $\pm 0.3\%$. By contrast, on phases L1 and L3 the same two meters track the reference closely at every current and power factor tested (within about ± 0.2 percentage points), confirming that the anomaly is confined to the L2 channel rather than reflecting a general single-phase-loading effect.

Figure 4 illustrates this same condition across all four test currents and shows that the deviation is stable in magnitude (roughly $+1.6\%$ to $+1.7\%$ for $\cos\varphi = 1$) and consistent between the two flagged meters, which is characteristic of a fixed calibration-coefficient error on the affected current channel rather than of random measurement noise. Under capacitive power factor $\cos\varphi = 0.8$ the deviation is larger still, reaching approximately $+2.5\%$ to $+2.8\%$ for #22 and #34 while the reference meter stays below $\pm 0.3\%$ throughout. Similar to the previous test, the flagged meters under inductive load show a smaller value and a different sign, consistent with the power-factor-dependent metrological response of static meters documented under nonsinusoidal test conditions [17].

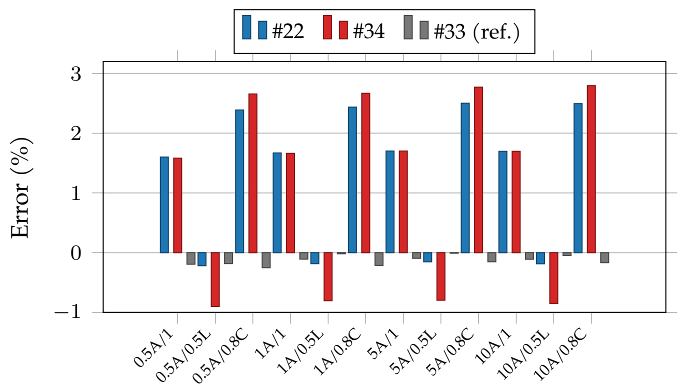

Figure 4. Registration error vs. current for single-phase load on L2.

This addresses objective (ii) of Section 3.1—assessing performance under load conditions that more closely resemble those found on the distribution network—and the magnitude of the observed offset is of the same order as the metrological imperfections reported for smart energy meters tested under non-idealized, more realistic signal conditions [6].

The effect of this error is even more pronounced in the interruption-of-phase- voltage test (IEC 62052-11:2022, Clause 9.4.5), applied in turn to each phase with the

Table 7. Error (%), single-phase load, $\cos\varphi = 1$, 0.5 inductive, 0.8 capacitive.

Meter	Phase	0.5 A			1 A			5 A			10 A		
	load	1	0.5L	0.8C	1	0.5L	0.8C	1	0.5L	0.8C	1	0.5L	0.8C
#22		−0.136	−0.188	−0.172	−0.083	−0.142	−0.054	−0.029	−0.137	−0.004	−0.048	−0.200	0.005
#34	L1	−0.184	−0.188	−0.235	−0.160	−0.155	−0.182	−0.114	−0.116	−0.127	−0.107	−0.136	−0.107
#33 (ref.)		−0.180	−0.189	−0.190	−0.096	−0.095	−0.150	−0.061	−0.052	−0.063	−0.067	−0.104	−0.056
#22		1.600	−0.218	2.388	1.669	−0.184	2.436	1.701	−0.153	2.501	1.696	−0.186	2.495
#34	L2	1.581	−0.901	2.656	1.662	−0.804	2.667	1.701	−0.797	2.770	1.696	−0.850	2.796
#33 (ref.)		−0.194	−0.183	−0.252	−0.109	−0.018	−0.214	−0.095	−0.010	−0.152	−0.111	−0.048	−0.167
#22		−0.175	−0.275	−0.198	−0.115	−0.112	−0.169	−0.064	−0.074	−0.058	−0.061	−0.102	−0.042
#34	L3	−0.216	−0.289	−0.320	−0.198	−0.128	−0.271	−0.149	−0.106	−0.180	−0.148	−0.155	−0.165
#33 (ref.)		−0.213	−0.309	−0.233	−0.192	−0.211	−0.194	−0.128	−0.138	−0.140	−0.128	−0.176	−0.124

Table 8. Error (%), interruption of two phase voltages, $\cos\varphi = 1$, 0.5 inductive, 0.8 capacitive.

Meter	Phase	0.5 A			1 A			5 A			10 A		
	load	1	0.5L	0.8C	1	0.5L	0.8C	1	0.5L	0.8C	1	0.5L	0.8C
#22		−0.134	−0.189	−0.124	−0.053	−0.154	−0.050	−0.024	−0.171	0.031	−0.030	−0.238	0.040
#34	L1	−0.182	−0.185	−0.205	−0.136	−0.180	−0.177	−0.098	−0.139	−0.083	−0.099	−0.174	−0.083
#33 (ref.)		−0.169	−0.180	−0.180	−0.085	−0.154	−0.096	−0.045	−0.107	−0.032	−0.050	−0.142	−0.032
#22		3.100	1.417	3.615	3.109	1.502	3.685	2.996	1.445	3.603	3.152	1.363	3.776
#34	L2	3.083	0.755	3.889	3.095	0.838	3.974	2.996	0.773	3.899	3.173	0.670	4.104
#33 (ref.)		0.238	0.198	0.029	0.245	0.326	0.139	0.164	0.211	0.009	0.289	0.209	0.172
#22		1.134	1.353	0.961	1.164	1.476	0.945	1.151	1.579	1.094	1.179	1.493	1.021
#34	L3	1.075	1.339	0.870	1.073	1.480	0.826	1.054	1.562	0.977	1.088	1.417	0.927
#33 (ref.)		0.049	−0.025	0.022	0.067	0.116	−0.021	0.063	0.220	0.129	0.450	0.103	0.043

other two de-energized as if interrupted. When the active phase is L2, meters #22 and #34 register errors of approximately +3.0% to +3.8% (#22) and +3.1% to +4.1% (#34) (Table 8) depending on current and power factor, roughly 1.5 to 2 times the deviation seen under single-phase L2 loading (Table 7), while reference meter #33 stays within ±0.45%.

Interestingly, when the active phase is L3 the two flagged meters also show a smaller but clearly non-negligible elevated error of about +1.0% to +1.6%, well above their own L1 results (within about ±0.24%) and above reference meter #33's L3 results (below ±0.45%). This secondary effect on L3, while much smaller than the primary L2 fault, is not fully explained by the present dataset; a possible contributing mechanism is cross-channel coupling within the meter's signal-processing chain under single-phase excitation, a phenomenon consistent with the power-factor-dependent metrological behavior of static meters reported in [17]. Confirming the underlying cause is left as an open question for a dedicated follow-up investigation.

Figure 5 compares the mean error of each meter under the standard balanced test versus the extended single-phase test versus the interruption of two phase voltages with load on L2. The reference meter's mean error is essentially unchanged between conditions, whereas #22 and #34 shift from a small positive bias (comparable to the reference) under balanced loading to a clearly elevated, consistent offset once the load is confined to the affected phase.

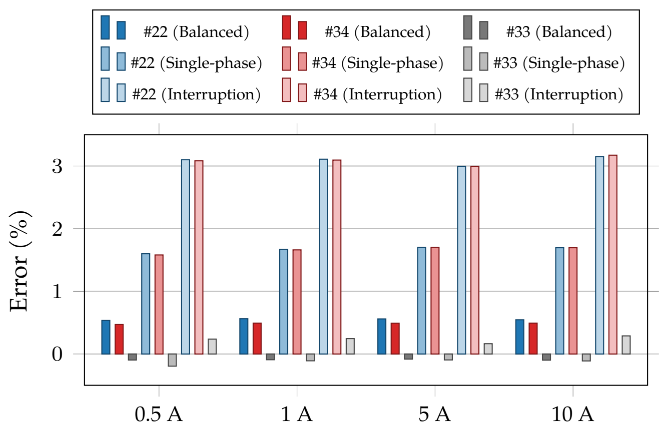

Figure 5. Mean registration error under the standard balanced test versus the extended single-phase (L2) test versus interruption of the phase voltage (load on L2, $\cos\varphi = 1$).

As shown in Table 9, symmetrical voltage variation

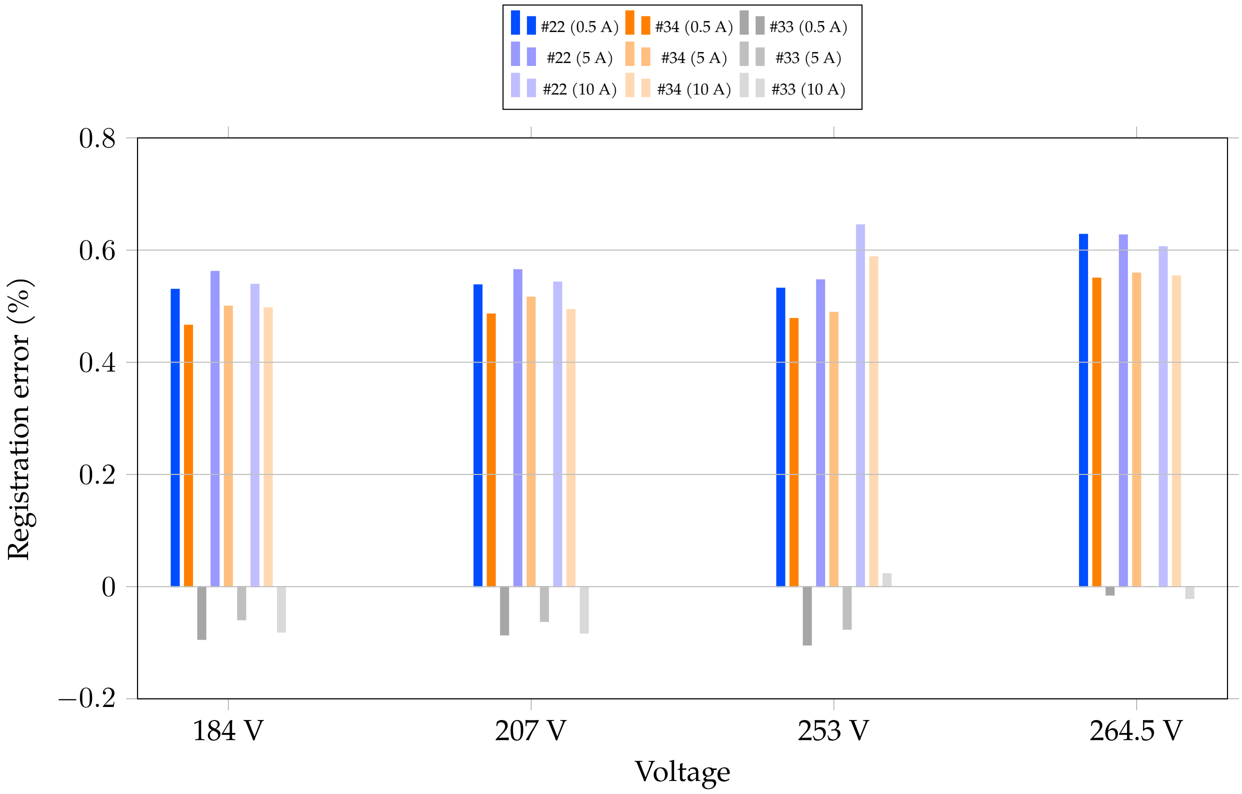

Figure 6. Mean registration error under variation of the balanced 3-phase voltage with 3-phase load ($\cos\varphi = 1$).

Table 9. Error (%), balanced 3-phase voltage variation with 3-phase load, $\cos\varphi = 1$.

Voltage	Meter	0.5 A	5 A	10 A
184 V	#22	0.530	0.562	0.539
	#34	0.466	0.500	0.497
	#33 (ref.)	−0.094	−0.059	−0.081
207 V	#22	0.538	0.565	0.543
	#34	0.486	0.516	0.494
	#33 (ref.)	−0.086	−0.062	−0.083
253 V	#22	0.532	0.547	0.645
	#34	0.478	0.489	0.588
	#33 (ref.)	−0.104	−0.076	0.023
264.5 V	#22	0.628	0.627	0.606
	#34	0.550	0.559	0.554
	#33 (ref.)	−0.015	0.000	−0.021

across the extended range (3×184 V to 3×264.5 V) under balanced three-phase load produces only a modest, gradual shift in registration error for #22 and #34 (approximately 0.47% to 0.65%), most visible at the two highest current/voltage combinations, while reference meter #33 remains within $\pm 0.10\%$ throughout. Unlike the single-phase L2 condition, voltage variation alone does not reproduce the elevated error signature, indicating that the fault is not voltage-sensitive and is not attributable to external conducted disturbances of the kind reported in [12]. The increase is essentially monotonic with voltage for both units—from about 0.47%–0.53% at 184 V to about 0.55%–0.63% at 264.5 V—a shift of roughly 0.1 percentage points across the full extended voltage range, an order of magnitude smaller than the 1.6%–4.1% offset associated with single-phase or phase-interruption loading on L2. Figure 6 plots the mean registration error over the extended balanced voltage range for the three meters.

Table 10 demonstrates that the registration error tracks the current magnitude specifically on phase L2, independent of overall load level: reordering the three columns by ascending L2 current (0.5 A, 5 A, 10 A), the error of #22 rises from $+0.055\%$ to $+0.565\%$ to $+1.139\%$, and that of #34 from -0.014% to $+0.504\%$ to $+1.112\%$, reaching a level comparable to pure single-phase L2 loading (Table 7) at 10 A, while reference meter #33 remains within a narrow band (-0.06% to -0.02%) regardless of current distribution. This confirms that the anomaly is localized to the L2 measurement channel rather than to load asymmetry in general.

Figure 7 illustrates the data shown in Table 10 and clearly shows the difference in errors at different current values on phase L2.

Table 10. Error (%), balanced 3-phase voltage, variation of load per phase, $\cos\varphi = 1$.

Meter	0.5-5-10 A	10-0.5-5 A	5-10-0.5 A
#22	0.565	0.055	1.139
#34	0.504	−0.014	1.112
#33 (ref.)	−0.063	−0.034	−0.023

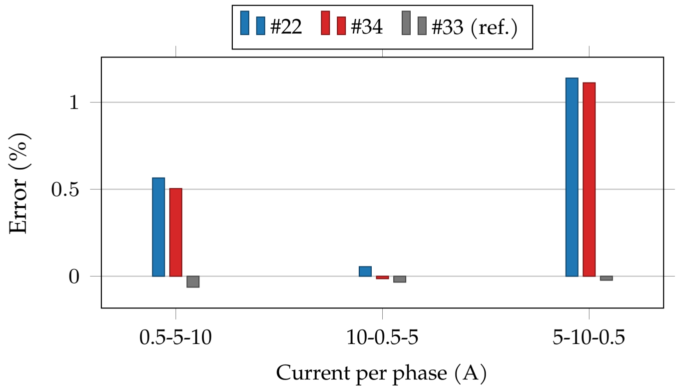

Figure 7. Mean registration error under balanced 3-phase voltage with 3-phase unbalanced load ($\cos\varphi = 1$).

Table 11 shows that introducing voltage asymmetry (184–230–254 V per phase) does not materially alter the relationship between registration error and the current flowing through phase L2. For the two tested current distributions, the errors of meters #22 and #34 remain close to those observed under the corresponding balanced-voltage conditions in Table 10, while the reference meter #33 remains near zero. This comparison suggests that voltage asymmetry does not substantially amplify the observed fault signature; the dominant change remains associated with the current magnitude on the L2 channel. This comparison is illustrated in Figure 8.

Table 11. Error (%), unbalanced 3-phase voltage and variation of load per phase, $\cos\varphi = 1$.

	Voltage 184-230-254 V per phase	
Meter	0.5-5-10 A	10-0.5-5 A
#22	$0.565^{\ddagger}$	$0.055^{\ddagger}$
#34	$0.504^{\ddagger}$	$-0.014^{\ddagger}$
#33 (ref.)	$-0.063^{\ddagger}$	$-0.034^{\ddagger}$

‡Values identical to those in Table 10 within measurement resolution; the unbalanced-voltage condition produced no statistically distinguishable change in registration error for any of the three meters.

Subsequent investigation of the two flagged units confirmed that the calibration coefficient recorded for the affected current channel differed from the correct value; correcting it restored agreement with the reference meter across all test points. Because the deviation only becomes clearly visible once the load is concentrated on the affected phase, it would very likely have gone unnoticed under the standard balanced test sequence alone—both units would have passed the routine accredited verification and been delivered to the customer. This is precisely the case that the AI-based screening of aggregated laboratory results was able to catch: by comparing each meter's error pattern against the population of otherwise-passing units, the two units with the anomalous signature were identified for targeted extended testing before dispatch. This result substantiates objective (iii) of Section 3.1: it demonstrates, on a real production case, that statistical screening of aggregated verification data can flag units requiring closer inspection before they would otherwise leave the verification process—consistent with the broader body of machine-learning-based anomaly-detection work on smart-meter data [8, 11], but applied here, unusually, to structured, standards-based verification results rather than to raw consumption time series.

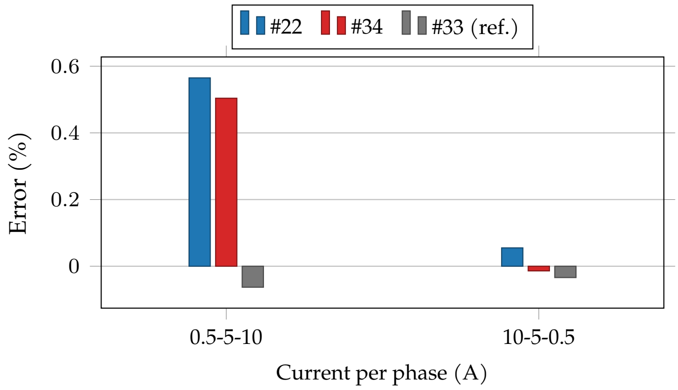

Figure 8. Mean registration error under unbalanced 3-phase voltage with 3-phase unbalanced load ($\cos\varphi = 1$).

6 Conclusion

This paper compared standard IEC 62052-11 / EN 50470-3 factory verification of three-phase smart meters against an extended set of validation conditions designed to approximate real distribution-network operating states—the extended verification methodology constituting the primary contribution of this work. It further evaluated whether statistical/AI-based screening of aggregated laboratory verification results can flag units requiring closer inspection before standard testing alone would have cleared them. The results show that a calibration fault confined to a single current channel can remain hidden under standard balanced verification—with a deviation of only a few tenths of a percent from the reference meter—while producing a repeatable registration-error signature on the order of 1.6% to 2.8% once the load is concentrated on the affected phase, tracking current magnitude on that phase specifically rather than voltage variation or general load asymmetry. Screening of the laboratory's aggregated verification results correctly flagged both affected units before the fault was independently confirmed by extended testing and traced to an incorrectly recorded calibration coefficient, preventing meters with this fault from being classified as fully compliant under standard testing alone.

Extending routine Type C verification with the proposed single-phase and phase-interruption test points would increase per-unit test duration. For an accredited inspection body such as EWG Control – Bor, this implies incremental effort in test-procedure calibration, which should be weighed against the demonstrated risk of channel-specific faults passing undetected under standard balanced verification alone.

These findings support extending routine Type C verification procedures with a small set of unbalanced/single-phase test points, and motivate further development of the anomaly-screening method—including its detection sensitivity, false-positive rate and integration into the laboratory's data pipeline—which will be presented in a dedicated follow-up paper. Future work will also address the integration of such screening into smart-grid-connected metering infrastructure for continuous, rather than point-in-time, validation.

Data Availability Statement

The verification data supporting the findings of this study are available from the author upon reasonable request. The internal EWG quality-system procedure UP.063 is a non-published document.

Funding

This work received no external funding.

Conflicts of Interest

The author is employed by EWG doo Belgrade, the manufacturer of the smart meters evaluated in this study; the accredited inspection body (EWG Control – Bor) and the internal verification procedure (UP.063) discussed herein also belong to EWG. The study was conducted using the company's laboratory facilities. EWG doo Belgrade was aware of this study and its submission for publication. The author declares this employment relationship as a potential competing interest and affirms that the measurements and analyses were carried out and reported objectively.

AI Use Statement

The author declares that no generative AI was used in the preparation of this manuscript.

Ethical Approval and Consent to Participate

Not applicable. This study involved laboratory testing of electricity-metering devices only and did not involve any human participants or animals.

References

[1] European Commission. (2021). *'Fit for 55': Delivering the EU's 2030 Climate Target on the Way to Climate Neutrality* (COM(2021) 550 final). Brussels: European Commission. Retrieved from https://www.eesc.europa.eu/en/our-work/opinions-information-reports/opinions/fit-55-delivering-eus-2030-climate-target-way-climate-neutrality

[2] European Commission. (2022). *REPowerEU Plan* (COM(2022) 230 final). Brussels: European Commission. Retrieved from https://eur-lex.europa.eu/resource.html?format=PDF&uri=cellar:fc930f14-d7ae-11ec-a95f-01aa75ed71a1.0001.02/DOC_1

[3] International Electrotechnical Commission. (2022). *Electricity metering equipment - General requirements, tests and test conditions - Part 11: Metering equipment* (IEC 62052-11:2022). Geneva: IEC. Retrieved from https://standards.iteh.ai/catalog/standards/clc/23606e6f-f5a6-4c89-9a42-a1a55b7357af/en-iec-62052-11-2021-a11-2022

[4] International Electrotechnical Commission. (2022). *Electricity metering equipment - Particular requirements - Part 22: Static meters for active and reactive energy* (IEC 62053-21:2022, IEC 62053-22:2022, IEC 62053-24:2022). Geneva: IEC. Retrieved from https://webstore.iec.ch/en/publication/29987

[5] CENELEC. (2022). *Electricity metering equipment (a.c.) — Part 3: Particular requirements — Static meters for active energy* (EN 50470-3:2022). Brussels: CENELEC. Retrieved from https://standards.iteh.ai/catalog/standards/clc/d898d898-a575-4387-8b76-e12cddca928f/en-50470-3-2022

[6] Bracale, A., Janowicz, J., Kuwałek, P., & Wiczyński, G. (2026). Challenges in the Proper Metrological Verification of Smart Energy Meters. *arXiv preprint arXiv:2601.16612*. [CrossRef]

[7] Korakianitis, N. S., Papageorgas, P., Vokas, G. A., Piromalis, D. D., Kaminaris, S. D., Ioannidis, G. C.,

& Zuazola, A. O. D. (2025). Design and Evaluation of a Research-Oriented Open-Source Platform for Smart Grid Metering: A Comprehensive Review and Experimental Intercomparison of Smart Meter Technologies. *Future Internet*, *17*(9), 425. [CrossRef]

[8] Amirkhanova, G., Aidynuly, A., Adilzhanova, S., Fu, Y., Dina, B., & Alipbeki, O. (2026). A comparative analysis of machine learning models for anomaly detection in industrial smart meter time-series data. *Information*, *17*(2), 131. [CrossRef]

[9] Guato Burgos, M. F., Morato, J., & Vizcaíno Imacaña, F. P. (2024). A review of smart grid anomaly detection approaches pertaining to artificial intelligence. *Applied Sciences*, *14*(3), 1194. [CrossRef]

[10] Zhang, J. E., Wu, D., & Boulet, B. (2021, October). Time series anomaly detection for smart grids: A survey. In *2021 IEEE electrical power and energy conference (EPEC)* (pp. 125-130). IEEE. [CrossRef]

[11] Patrizi, G., Garzon Alfonso, C., Calandroni, L., Bartolini, A., Iturrino Garcia, C., Paolucci, L., ... & Ciani, L. (2024). Anomaly detection for power quality analysis using smart metering systems. *Sensors*, *24*(17), 5807. [CrossRef]

[12] Leferink, F., Keyer, C., & Melentjev, A. (2017). Static energy meter errors caused by conducted electromagnetic interference. *IEEE electromagnetic compatibility magazine*, *5*(4), 49-55. [CrossRef]

[13] European Parliament and Council. (2014). *Directive 2014/32/EU of 26 February 2014 on the harmonisation of the laws of the Member States relating to the making available on the market of measuring instruments* (MID). Official Journal of the European Union. Retrieved from https://eur-lex.europa.eu/eli/dir/2014/32/oj/eng

[14] Ministry of Economy of the Republic of Serbia. (2024).*Regulation on the verification of active electrical energy meters of accuracy classes A, B, C, 2, 1 and 0.5 S* (in Serbian). Official Gazette of the Republic of Serbia, No. 14/2024. Retrieved from https://www.dmdm.rs/sr/vesti/pravilnik-o-overavanju-brojila-aktivne-elektricne-energije-klase-tacnosti-a-b-c-2-1-i-0-5-s

[15] International Organization for Standardization. (2012). *Conformity assessment - Requirements for the operation of various types of bodies performing inspection* (ISO/IEC 17020:2012). Geneva: ISO. Retrieved from https://www.iso.org/standard/52994.html

[16] GFUVE Group. (2026). *GF302D - Portable three-phase kWh meter test equipment* [Datasheet]. Retrieved from https://www.gfuvegroup.com/pdf/GF302D.pdf

[17] Cataliotti, A., Cosentino, V., Lipari, A., & Nuccio, S. (2008). Metrological characterization and operating principle identification of static meters for reactive energy: an experimental approach under nonsinusoidal test conditions. *IEEE Transactions on Instrumentation and Measurement*, *58*(5), 1427-1435. [CrossRef]

Saša Aleksandrov was born in Serbia in 1972. He graduated from the Faculty of Electronic Engineering, University of Niš, in 1997. During 1998 and 1999 he worked as a research assistant at the Faculty of Electronic Engineering, Department of Power Engineering, Laboratory for Electric Machines and Drives. His main research interests include electrical measurements, smart electricity meters, the development and production of communication modules, and electric power networks. He is currently an engineer at EWG. (Email: alsasa@ewg.rs)